

## Beam Action Spectroscopy via Inelastic Scattering<sup>†</sup>

Bobby H. Layne and Liam M. Duffy\*

Department of Chemistry & Biochemistry, University of North Carolina at Greensboro,  
Greensboro, North Carolina 27402

Hans A. Bechtel, Adam H. Steeves, and Robert W. Field

Department of Chemistry, Massachusetts Institute of Technology, Cambridge, Massachusetts 02139

Received: January 31, 2007; In Final Form: April 10, 2007

In this article, a new technique we call Beam Action Spectroscopy via Inelastic Scattering (BASIS) is demonstrated. BASIS takes advantage of the sensitivity of rotational state distributions in a supersonic molecular beam to inelastic scattering within the beam. We exploit BASIS to achieve increased sensitivity in two very different types of experiments. In the first, the UV photodissociation spectrum of OCIO is recovered by monitoring intensity changes in the pure rotational transition of a spectator molecule (OCS) downstream from the nozzle, revealing a new vibrational structure in the region between 30 000 and 36 000  $\text{cm}^{-1}$ . In the second, the mid-IR vibrational spectrum of acetylene is recorded simply by monitoring a single pure rotational transition of OCS co-expanded with acetylene. The technique may prove particularly fruitful when an excitation process produces product dark states that are not easily probed by conventional spectroscopy.

### 1. Introduction

The use of supersonic molecular beams in molecular spectroscopy has become a mainstay of modern high-resolution spectroscopic methods. The rotational and vibrational state distributions of molecules seeded in a supersonic molecular beam are exceedingly narrow and cold, providing a significant reduction in spectral congestion over room-temperature gas cell experiments. The nearly mono-energetic nature of the molecular beam flux has been used to great effect in the infrared optothermal detection technique pioneered by Gough, Miller, and Scoles,<sup>1,2</sup> whereby the molecular beam itself is directed onto a liquid-helium-cooled bolometer placed inside a vacuum chamber. In that technique, very small increases in the energy flux of the molecular beam hitting the bolometer may be exploited as a sensitive indicator of when molecules in the beam absorb infrared radiation. Similarly, decreases in the energy flux are observed when the infrared absorption leads to dissociation and the subsequent loss of fragment molecules or atoms from the beam.

In this article, a new method is demonstrated that uses the rotational distribution of molecules in the beam as a “virtual” bolometer for detecting energetic processes that occur within the molecular beam. Analogous to the optothermal detection technique, absorption of radiation or fragmentation of molecules and/or clusters may be indirectly detected by their action on inelastic scattering within the beam and by the resulting changes to the rotational distribution of a “reporting” molecule within the beam. Specifically, action spectra are obtained by monitoring changes in rotational line intensities of the reporting spectator molecule. The technique relies on the fact that the probed rotational state populations of the reporting molecule are very sensitive ( $\propto T^{-2}$ ) to the rotational temperature in the beam. Because of this sensitivity, when a parent molecule seeded in

the molecular beam absorbs radiation and undergoes fragmentation, subsequent collisions with a spectator reporting molecule can result in measurable changes to the reporting molecule’s rotational temperature. Furthermore, a gain effect is observed whereby the rotational line intensity changes are significantly larger than those predicted in traditional “hole-burning” experiments (i.e., greater than the product of laser fluence and UV absorption cross sections) because a single parent absorption event can lead to a cascade of collisions with multiple reporting molecules. We have given this technique the acronym BASIS, which is short for Beam Action Spectroscopy via Inelastic Scattering.

In this article we demonstrate the use of the BASIS technique in two very different experiments: (1) to reveal previously unreported vibrational structure in the UV spectrum of OCIO between 30 000 and 36 000  $\text{cm}^{-1}$ , and (2) to record the mid-IR vibrational spectrum of acetylene.

It can be shown that the methodology employed in the BASIS technique is quite general; the effects should be observable by many high-resolution probe techniques. We suggest that it may prove particularly useful when the process and products studied are dark to conventional spectroscopic techniques, such as the production of long-lived excited triplet electronic states.

### 2. Experimental Methods

The experiments discussed in this article were carried out separately at UNCG and MIT using similar experimental setups that have previously been described.<sup>3–5</sup> The UV photodissociation studies on OCIO were undertaken at UNCG, while the IR vibrational spectrum of acetylene was recorded at MIT. Common to both instruments is the use of a CW millimeter/submillimeter-wavelength (mm/submm-wave) radiation apparatus in a direct absorption configuration. Changes in the pure rotational line intensities of a reporting molecule such as OCS were observed as variations in transmitted mm/submm-wave

<sup>†</sup> Part of the “Roger E. Miller Memorial Issue”.

\* Corresponding author. E-mail: Liam\_Duffy@uncg.edu.

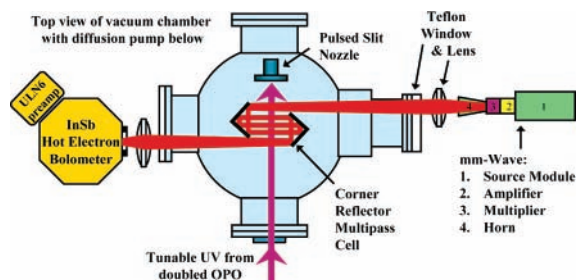


**Figure 1.** Overview of experimental geometry employed in the UV photodissociation of OCIO.

power incident on a liquid-helium-cooled InSb hot electron bolometer. As will be discussed, pure rotational transitions offer some sensitivity advantage but are not a requirement of the BASIS technique; any high-resolution spectroscopic technique that can be used to monitor the population of a rotational state in the beam will work.

**2.1. Photodissociation Setup.** In the UNCG photodissociation experiment (see Figure 1), mm/submm-wave frequencies ranging from 50 to 330 GHz were employed. Frequencies from 50 to 110 GHz were generated by millimeter-wave “source modules” from Agilent Technologies (models 83557A and 83558A covering 50–75 GHz and 75–110 GHz, respectively), which were driven by a high-power microwave synthesizer (Agilent model HP83623B). The output of the source modules in turn could be multiplied to frequencies between 110 and 330 GHz with a combination of solid-state millimeter-wave amplifiers and Schottky diode multipliers.<sup>3</sup> Tunable UV radiation from a pulsed (10 Hz) Nd:YAG pumped OPO laser (Continuum: model Panther EX) was either counter-propagated collinearly with the molecular beam or crossed perpendicularly downstream from a pulsed slit jet nozzle (Parker Hannifin Corp., General Valve Division Series 97) with slit dimensions of 150  $\mu\text{m}$  by 1.2 cm. The nozzle was pulsed at 10 Hz, and typical gas pulses were 300–500  $\mu\text{s}$  long. The mm/submm-wave probe radiation was passed CW and perpendicular to the molecular beam and downstream from the nozzle. In some experiments, corner reflectors were used to multipass the millimeter waves 5 times through the molecular beam.

When the mm/submm-wave frequency is set to a known transition of the parent, product, or reporting molecule, a transient absorption signal is detected by the bolometer and then recorded with a digital oscilloscope and subsequently downloaded to a computer. In the case of photolysis-generated product molecules, this transient absorption is observed for a short period of time following the laser flash, while in the case of a parent or reporting molecule, the absorption signal lasts for the duration of the gas pulse. The UV laser pulse was timed to coincide with the center of the gas pulse and revealed itself in the parent or reporting molecule’s absorption signals either as a “hole” when low- $J$  states are probed or as a “buildup” following the laser flash when high- $J$  states are probed. The hole versus buildup effect reflects the Boltzmann population shift to higher energies and is demonstrated and discussed in section 3.1. With this setup it is possible to scan either the millimeter waves or the UV laser. In the latter case, the UV action spectrum for the creation of fragments can be observed by monitoring the depth of the hole as a function of UV wavelength.

In these experiments, OCIO was generated in a more reproducible fashion than described in our earlier work.<sup>3</sup> Instead of bubbling a  $\text{Cl}_2/\text{He}/\text{Ar}$  premix (10%, 45%, and 45% partial pressures, respectively) through water and then sodium chlorite powder mixed with sand, the bubbling step was omitted

altogether. Rather, a few milliliters of water were squirted every couple days directly onto the sodium chlorite powder/sand mixture. It should be noted that care must be taken in generating OCIO that explosive concentrations are not generated.<sup>6</sup> When OCS was used as the reporting molecule, it was combined with the gas premix at a partial pressure of 10%, with typical stagnation pressures around 300 Torr.

**2.2. Vibrational Spectroscopy Setup.** The acetylene vibrational spectrum observed with the BASIS technique was performed in a previously described instrument at MIT.<sup>4,5</sup> The molecular beam was generated by expanding a gas mixture consisting of 3% OCS, 22%  $\text{C}_2\text{H}_2$ , and 75% Ar into a vacuum chamber with a 1 mm diameter orifice pinhole pulsed valve (Parker Hannifin Corp., General Valve Division, Series 9). Typical stagnation pressures were between 2 and 3 atm. The CW millimeter-wave radiation was produced by a W-band (72–106 GHz) Gunn oscillator (J. E. Carlstrom Co.) that was phase-locked (XL Microwave 800A) to the 10th harmonic of a microwave synthesizer (HP 8673E) and coupled through waveguide components to a calibrated attenuator (Hitachi W9513). Higher frequencies were generated by doubling (144–212 GHz) and tripling (216–318 GHz) the output of the Gunn oscillator in Schottky diode multipliers (Virginia Diodes). The radiation was emitted into free space orthogonal to the molecular beam through a standard gain pyramidal horn (TRG Control Data, 15 dB). A pair of PTFE lenses ( $f = 40$  cm,  $f = 30$  cm) focused the millimeter-wave radiation to a spot size of  $\sim 1$  cm diameter at the point of intersection with the molecular beam  $\sim 2$  cm downstream from the nozzle. After exiting the chamber through a PTFE window, the millimeter-wave beam was refocused by a second pair of PTFE lenses ( $f = 30$  cm,  $f = 40$  cm) onto a liquid-helium-cooled InSb hot electron bolometer (Cochise Instruments). The bolometer output was digitized with a 500 MHz oscilloscope (Lecroy LC334A) and transferred to a computer for storage.

The IR radiation required to vibrationally excite acetylene was generated in a two-step process involving difference-frequency generation (DFG) and optical parametric amplification (OPA) in  $\text{LiNbO}_3$ . Approximately 1 mJ per pulse of mid-IR light at 3  $\mu\text{m}$  was first generated via DFG by combining the 1.064  $\mu\text{m}$  fundamental of a  $\text{Nd}^{3+}$ :YAG laser (Spectra Physics PRO270) with the output of a dye laser (Lambda Physik FL2002, Exciton LDS 790) in a  $\text{LiNbO}_3$  crystal housed in an auto tracking unit (Quanta-Ray WEX-1). The 3  $\mu\text{m}$  radiation was then amplified to approximately 3 mJ per pulse in an OPA stage consisting of a  $\text{LiNbO}_3$  crystal (INRAD) pumped by another 1.064  $\mu\text{m}$  beam. The unfocused IR light was counter-propagated collinearly with the molecular beam and entered the vacuum chamber through a  $\text{CaF}_2$  window oriented at Brewster’s angle.

### 3. Results and Discussion

**3.1. Electronic and Vibrational Spectroscopy with the BASIS Technique. Photodissociation.** The use of mm/submm-wave spectroscopy to probe the photodissociation of OCIO has been presented recently as a test-case system for demonstrating the capabilities of the molecular beam instrument at UNCG.<sup>3</sup> In this previous publication, mm/submm-wave radiation was tuned to a strong rotational hyperfine transition of OCIO and then the UV laser was set to wavelengths previously assigned<sup>7</sup> to predissociative pure symmetric stretching modes of the parent. When resonant, the UV laser created a “hole” in the parent mm/submm-wave absorption signal that was originally assumed to be the direct loss of parent molecules through UV photodisso-

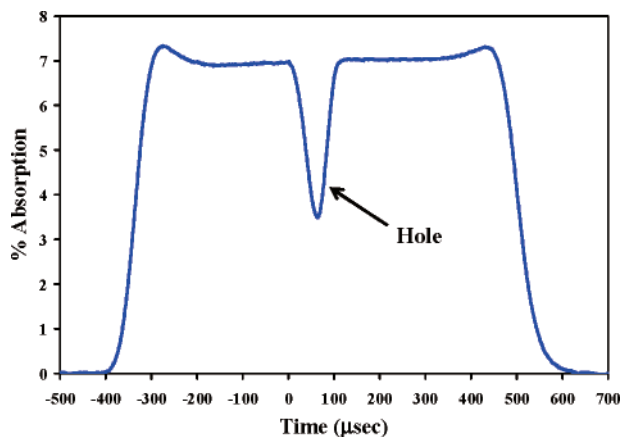


**Figure 2.** A millimeter-wave absorption time trace centered on a single hyperfine line of  $\text{O}^{35}\text{ClO}$  ( $N = 6 \leftarrow 5$ ,  $J = 6^{1/2} \leftarrow 5^{1/2}$ ,  $K_{-1} = 3 \leftarrow 2$ ,  $K_{+1} = 4 \leftarrow 3$ ,  $F = 8 \leftarrow 7$ ) as it is pulsed into the vacuum chamber (initially reported in ref 3). The “hole” following the laser pulse at time zero shows a 50% depletion of the parent signal when only an 8.4% depletion is expected from the laser fluence and UV cross section.

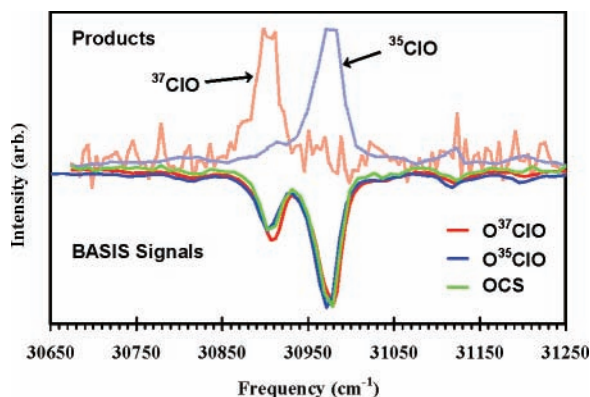


**Figure 3.** Action spectra obtained by scanning the UV laser while monitoring a single rotational hyperfine transition in OCIO, ClO, or OCS. The positive going signals were obtained by monitoring rotational hyperfine transitions ( ${}^2\Pi_{3/2}$ ,  $v = 0$ ,  $J = 8^{1/2} \leftarrow 7^{1/2}$ ,  $F = 10 \leftarrow 9$ ,  $\Lambda = 1\phi - 1$ ) of the  $^{35}\text{ClO}$  and  $^{37}\text{ClO}$  product isotopologues, while the negative-going BASIS signals were obtained by monitoring the depth of the reporting molecule’s absorption “hole” as a function of UV wavelength. The BASIS signals are nearly the same for OCS ( $J = 8\phi 7$ ) and the parent isotopologues. The parent  $\text{O}^{35}\text{ClO}$  and  $\text{O}^{37}\text{ClO}$  hyperfine transitions used were at 268797.6550 and 262085.4431 MHz, respectively (corresponding to  $N = 3 \leftarrow 2$ ,  $J = 3^{1/2} \leftarrow 2^{1/2}$ ,  $K_{-1} = 3 \leftarrow 2$ ,  $K_{+1} = 0 \leftarrow 1$ ,  $F = 5 \leftarrow 4$ ).

ciation. We now know that this is only partially true. As pointed out in the earlier work, the so-called parent “hole-burning” signals (see Figure 2) that we observed were a factor of 6 times too deep to be accounted for by laser fluence and UV cross sections, an anomaly that was unexplained in the previous article.

In the current work, we demonstrate that the “hole-burning” spectra we previously reported reflect the loss of parent signal due primarily to inelastic collisions with atomic and molecular photofragments. The molecular beam density is sufficiently high that through multiple collision events, the photoproducts significantly alter the rotational population distribution of the parent molecules in the molecular beam and cause population in the low rotational states of the cold parent to be transferred to higher rotational states. The net effect is that low rotational states of the cold parent should be depleted and exhibit a “hole”, whereas high rotational states should show a buildup in signal.

Figure 3 shows an action spectrum obtained by scanning the

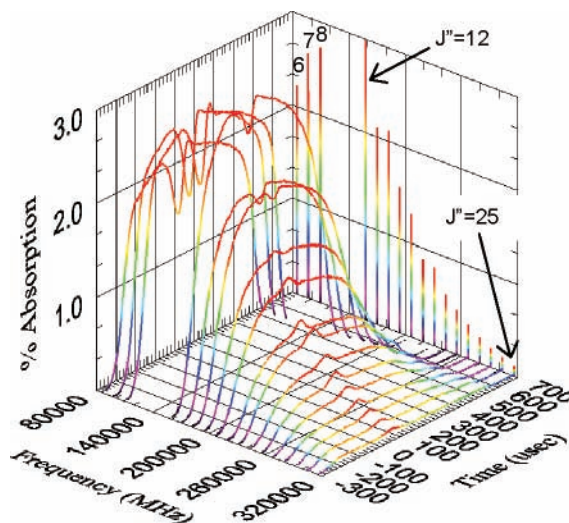


**Figure 4.** Experimental time traces demonstrating depletion and buildup in the pure rotational line intensities as a function of rotational state of a reporting molecule ( $\text{OCS } J'' = 6-8$  and  $J'' = 12-25$ ) seeded in a molecular beam containing parent OCIO. The UV laser is set to the predissociative  $\tilde{A}^2A_2$  ( $\nu_1 = 15$ )  $\leftarrow \tilde{X}^2B_1$  transition of  $\text{O}^{35}\text{ClO}$ .

UV laser frequency and monitoring a single rotational hyperfine transition in the parent molecules ( $\text{O}^{35}\text{ClO}$  or  $\text{O}^{37}\text{ClO}$ ) or in the product molecules ( $^{35}\text{ClO}$  or  $^{37}\text{ClO}$ ). As expected, the  $^{35}\text{ClO}$  and  $^{37}\text{ClO}$  molecules are produced only when the laser coincides with a transition originating from  $\text{O}^{35}\text{ClO}$  or  $\text{O}^{37}\text{ClO}$ , respectively. When the  $\text{O}^{35}\text{ClO}$  parent molecule is monitored, however, we observe a decrease in signal when the laser is coincident with  $\text{O}^{35}\text{ClO}$  transitions, as expected, but we also observe a decrease in signal when the laser is coincident with  $\text{O}^{37}\text{ClO}$  transitions. Likewise, when the  $\text{O}^{37}\text{ClO}$  parent molecule is monitored, we observe a decrease in signal when the laser is coincident with  $\text{O}^{35}\text{ClO}$  and  $\text{O}^{37}\text{ClO}$  transitions. Clearly, the “holes” in the parent molecule are arising from a different mechanism than the expected loss from direct dissociation.

Figure 3 demonstrates that monitoring a rotational transition of OCS seeded in the OCIO gas mixture yields an action spectrum that is identical to the spectra obtained by monitoring either isotope of the OCIO parent. This result indicates that molecules other than the photoactive molecule may be used to report on the rotational temperature of the molecular beam. Indeed, any molecule (including the undissociated parent itself) seeded in the molecular beam should display this behavior. Thus, the reporting molecule can be chosen to satisfy experimental conditions; that is, the reporter molecule should be inert, not photoactive in the region of interest, and in the case of millimeter-wave detection, should possess a permanent dipole moment. If the reporting molecule is also the parent molecule, then there is an additional component to the BASIS signal that is simply due to the expected loss of parent from dissociation. However, in the case of OCIO, the hole-burning signals appear to be dominated by the BASIS signal because the intensities of the  $\text{O}^{35}\text{ClO}$  and  $\text{O}^{37}\text{ClO}$  transitions have the same ratio, regardless of whether the  $\text{O}^{35}\text{ClO}$  or  $\text{O}^{37}\text{ClO}$  parent is monitored.

In Figures 4 and 5, the effect of rotational state changing collisions on the temperature profile of the molecular beam is demonstrated, showing both depletion and buildup in the BASIS signals. The spectra were recorded by fixing the UV laser wavelength to the  $\nu_1 = 15$  mode of  $\text{O}^{35}\text{ClO}$  (collinear with the molecular beam) while the mm/submm-waves were set to the known line center transition frequencies of OCS and multipassed through the molecular beam 5 times (perpendicular to the

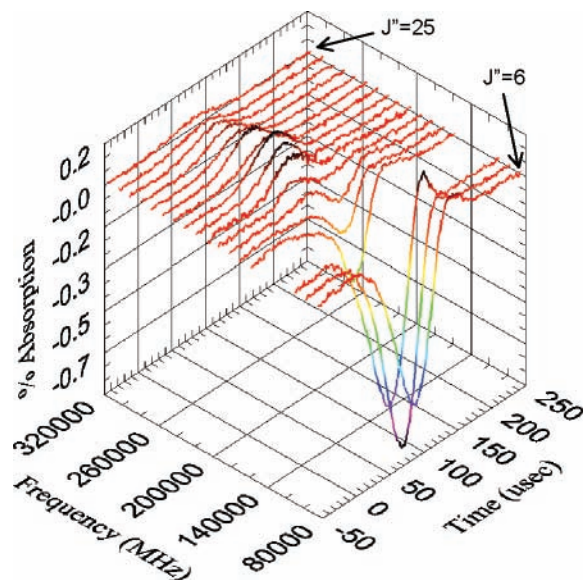


**Figure 5.** Experimental time traces showing only the change in absorption intensity of OCS following the laser pulse at time zero, that is, the “holes”. They show significant depletion of low- $J''$  rotational states and buildup in high- $J''$  rotational states (the frequency axis is inverted relative to Figure 4 to reduce the number of overlapped traces).

molecular beam and 4–10 cm downstream from the slit nozzle). In this experiment, the OCS reporting molecule is also mixed in at 10% concentration with the  $\text{Cl}_2/\text{He}/\text{Ar}$  premix. Figures 4 and 5 show the individual mm/submm-wave absorption time traces for a variety of OCS rotational transitions, ranging from  $J'' = 6$  to 8 and  $J'' = 12$  to 25. It is clear that for the low- $J''$  rotational transitions, depletion is observed following the laser pulse, while for high- $J''$  rotational transitions, a buildup is observed. These changes reflect an overall increase in the rotational temperature of the reporter molecule in the molecular beam. The line intensities before the laser fires can be used to determine the rotational temperature of the reporting molecule in the molecular beam. In this case, OCS was found to have a

rotational temperature of 22 K, although the temperature of the high-energy tail of the distribution is closer to 24 K, reflecting the fact that the molecular beam rotational distribution is not well described by a single temperature. By monitoring the intensity of the absorption signals at their deepest point in the time traces, a new rotational temperature for OCS in the molecular beam can be crudely estimated. The assumption here is that over the time window of the “hole”, the mm/submm-wave beam sampled only molecules that were in the excitation/thermalization region of the molecular beam. This new distribution showed only a small shift on the order of  $\sim 3$  K in the overall rotational temperature.

It can be shown that a shift of only +1 K in a rotational temperature distribution of a reporter molecule such as OCS may cause the most intense rotational line ( $J = 7 \leftarrow 6$  at  $T_{\text{rot}} = 22$  K) to diminish in intensity by as much as 6%. Assuming an experimental dynamic range on the order of 1 part in  $10^5$ , temperature shifts as small as 200  $\mu\text{K}$ , should be observable.

*Vibration (Mid-IR Spectrum of Acetylene).* Figure 6 demonstrates the use of the BASIS technique to measure the high-resolution mid-IR spectrum of acetylene by monitoring a rotational transition in OCS. In the previous example, the rotational temperature of the reporter molecule was altered by translationally hot product molecules from the photodissociation of OCIO. Acetylene, however, does not dissociate in the infrared, indicating that vibration–rotation transfer can contribute to BASIS signals in addition to translation–rotation transfer. We also wish to highlight the fact that acetylene transitions were detected with a pure rotational spectroscopic technique, despite the fact that acetylene does not possess a permanent dipole moment. This result emphasizes the point that the BASIS technique is a general method that is sensitive to all molecules and fragments, provided the probe method has the requisite sensitivity (inelastic scattering cross sections, etc.).

**3.2. UV Predissociative BASIS Spectrum of OCIO.** Over the last 15 years, the UV photodissociation spectrum of OCIO has been the focus of numerous studies aimed at determining the product channel pathways,<sup>8–15</sup> absorption cross sections,<sup>16</sup> dynamics,<sup>6,7,9,13,17–20</sup> and in turn, the significance of OCIO in

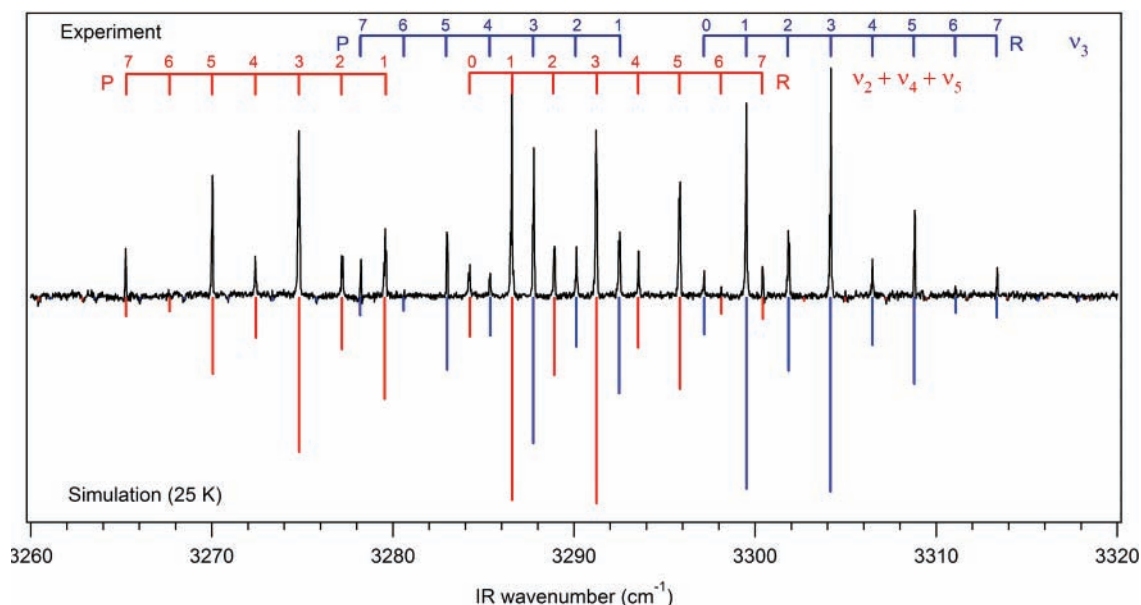


**Figure 6.** Vibration–rotation spectrum of acetylene observed with the BASIS technique. The spectrum was recorded by monitoring the change in intensity of a pure rotational transition of OCS ( $J = 7 \leftarrow 6$ ) seeded in the molecular beam with acetylene. The laser excitation and subsequent thermalization occurred in the high-density region near the nozzle, and the millimeter-wave absorption intensity change was monitored in the period immediately following the IR laser pulse.

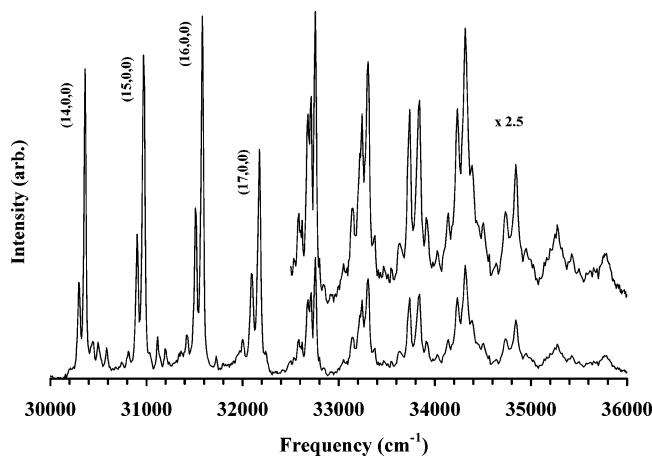


**Figure 7.** UV photodissociation BASIS spectrum of the  $\tilde{A}^2A_2 \leftarrow \tilde{X}^2B_1$  electronic transition in OCIO. The spectrum is obtained by monitoring the depth of the “hole” observed in the direct absorption signal of a hyperfine rotational transition of  $O^{35}ClO$  at 268797.6550 MHz ( $N = 3 \leftarrow 2$ ,  $J = 3\frac{1}{2} \leftarrow 2\frac{1}{2}$ ,  $K_{-1} = 3 \leftarrow 2$ ,  $K_{+1} = 0 \leftarrow 1$ ,  $F = 5 \leftarrow 4$ ). In this case, the parent molecule is also the reporting molecule and the signals have been inverted for clarity. The doublets ( $O^{37}ClO$ ,  $O^{35}ClO$ ) in the low-energy region of the spectrum correspond to a progression of symmetric stretching modes starting with  $\nu_1 = 14$ ; the other features have not been assigned.

the stratospheric ozone cycle.<sup>21,22</sup> In all of these studies, the dominant product pathway (>95%) has been found to be the production of ClO plus oxygen atoms.

At UV excitation energies below 30 000  $cm^{-1}$ , lower-energy regions of the excited  $\tilde{A}^2A_2$  electronic potential may be accessed. The spectrum exhibits a clean progression of predissociative normal mode combination bands ( $\nu_1, 0, 0$ ), ( $\nu_1, 0, 2$ ), ( $\nu_1, 1, 0$ ), and ( $\nu_1, 1, 2$ ) of the excited  $\tilde{A}^2A_2$  electronic state.<sup>23,24</sup>

Figure 7 shows the BASIS spectrum of OCIO in the range from 30 000 to 36 000  $cm^{-1}$  (333–278 nm). The spectrum in the range from 30 000 to 32 400  $cm^{-1}$  is dominated by the regular progression of symmetric stretching modes ( $\nu_1, 0, 0$ ). To the red of each of these dominant peaks is a smaller peak due to the chlorine-37 isotopologue of the parent OCIO molecule, as demonstrated by the  $^{37}ClO$  product signals in Figure 3. The spectrum has not been normalized with respect to laser power. It is worth noting that the weaker satellite transitions in between the dominant symmetric stretching modes in this region have yet to be assigned. It is not clear whether these smaller features simply reflect extensions of the normal mode combination bands that have been assigned lower down in the potential,<sup>23</sup> or whether a higher order level of vibrational analysis (polyads) is required. It is also worth noting that at energies above 32 400  $cm^{-1}$ , highly vibrationally inverted product distributions begin to appear<sup>7</sup> and that by 34 100  $cm^{-1}$  (UV wavelengths shorter than 293 nm), dramatically inverted product vibrational states of ClO ( $\nu > 19$ ) have been observed.<sup>25</sup> In the presence of molecular nitrogen, these vibrationally hot ClO products have even been shown to produce  $N_2O$ .<sup>26</sup>

The vibrational line widths of the peaks in Figure 7 are 30  $cm^{-1}$ , which is significantly larger than the 5  $cm^{-1}$  resolution of the UV output of the frequency-doubled OPO laser. We assume that the large line widths reflect the fact that the UV resolution, combined with lifetime broadening, is not adequate to uniquely excite individual rotational states of the OCIO parent and that the width of the vibrational bands in the BASIS spectrum reflects the entire unresolved ground-state rotational

manifold, which is roughly 30  $cm^{-1}$  wide, at molecular beam temperatures.

#### 4. Conclusions

The technique described in this article makes use of inelastic scattering in a molecular beam to measure the UV photodissociation action spectrum of OCIO in the high-energy region beyond 30 000  $cm^{-1}$ , where it reveals features that have not previously been assigned. In so doing, a new form of action spectroscopy is demonstrated that relies on the ability of rotational spectroscopy to detect small changes in the rotational state population distribution of a spectator/reporting molecule in a molecular beam. In Figure 5 of this article, this population shift is demonstrated as a “hole” in the absorption signal of low- $J''$  rotational states of the reporting molecule and a “buildup” at high- $J''$  rotational states. Though not presented here, similar depletion and buildup effects were observed (in both labs) in photodissociation studies of  $SO_2$ . The BASIS technique is further demonstrated in this current article by measuring the mid-IR vibration–rotation spectrum of acetylene by probing the rotational line intensity changes of OCS, seeded with acetylene in the molecular beam. We suggest that the technique may find particular utility in experiments with dark states, that is, states that cannot be observed by conventional spectroscopic techniques.

Under the conditions used to generate Figures 4 and 5 (i.e., OCS  $T_{rot} = 22$  K), the largest signal change is observed for  $J'' = 7$ . In this case, it can be shown that there is a modest (factor of  $\sim 1.8$ ) sensitivity advantage to probing rotational state population differences as opposed to probing the population of the lower state alone. However, any high-resolution spectroscopic technique that can probe populations of individual rotational states of a spectator molecule should suffice. The reporting molecule and rotational state should be chosen to provide the largest signal intensity, and the excitation process studied must produce fragments or species with excited-state lifetimes long enough (>microseconds) for inelastic scattering to thermalize the excitation energy. In the end, the sensitivity of any BASIS experiment will ultimately depend on the dynamic range available for probing the reporting molecule, the excitation cross section and power, the excited-state lifetimes, the inelastic collision cross sections, the molecular beam density, and the experimental geometry. With the dynamic range afforded by mm/submm-wave techniques discussed in this article, the BASIS technique should be sufficiently sensitive to reveal rotational temperature shifts of a reporting molecule as small as 200  $\mu K$ , making the technique highly sensitive to any energetic process that results in inelastic scattering within the molecular beam.

**Acknowledgment.** L.M.D. thanks Prof. Robert M. Whitnell for helpful conversations and undergraduate research assistants at UNCG: Brian P. Mehl, Joseph N. Krenicky, and Daphne L. Villanueva. H.A.B. acknowledges the Donors of the American Chemical Society Petroleum Research Fund for support, and A.H.S. acknowledges the Army Research Office for a National Defense Science and Engineering Graduate Fellowship. The work at MIT was supported by the Office of Basic Energy Sciences of the U.S. Department of Energy (DE-FG0287ER13671).

#### References and Notes

- (1) Gough, T. E.; Miller, R. E.; Scoles, G. *Appl. Phys. Lett.* **1977**, *30*, 338.

- (2) Miller, R. E. Infrared laser spectroscopy. In *Atomic and Molecular Beam Methods*; Scoles, G., Ed.; Oxford University Press: New York, 1992; Vol. 2, Chapter 6, p 192.
- (3) Duffy, L. M. *Rev. Sci. Instrum.* **2005**, *76*, 093104/1.
- (4) Bechtel, H. A.; Steeves, A. H.; Field, R. W. *Astrophys. J.* **2006**, *649*, L53.
- (5) Steeves, A. H.; Bechtel, H. A.; Coy, S. L.; Field, R. W. *J. Chem. Phys.* **2005**, *123*, 141102/1.
- (6) Baumert, T.; Herek, J. L.; Zewail, A. H. *J. Chem. Phys.* **1993**, *99*, 4430.
- (7) Furlan, A.; Scheld, H.; Huber, J. R. *J. Chem. Phys.* **1997**, *106*, 6538.
- (8) Davis, H. F.; Lee, Y. T. *J. Phys. Chem.* **1992**, *96*, 5681.
- (9) Davis, H. F.; Lee, Y. T. *J. Chem. Phys.* **1996**, *105*, 8142.
- (10) Lin, J. J.; Hwang, D. W.; Lee, Y. T.; Yang, X. *J. Chem. Phys.* **1998**, *108*, 10061.
- (11) Delmdahl, R. F.; Ullrich, S.; Gericke, K. H. *J. Phys. Chem. A* **1998**, *102*, 7680.
- (12) Hwang, D. W.; Lin, J. J.; Lee, Y. T.; Yang, X. *Proc. SPIE-Int. Soc. Opt. Eng.* **1998**, *3271*, 15.
- (13) Peterson, K. A.; Werner, H.-J. *J. Chem. Phys.* **1996**, *105*, 9823.
- (14) Bishenden, E.; Donaldson, D. J. *J. Chem. Phys.* **1994**, *101*, 9565.
- (15) Bishenden, E.; Donaldson, D. J. *J. Chem. Phys.* **1993**, *99*, 3129.
- (16) Wahner, A.; Tyndall, G. S.; Ravishankara, A. R. *J. Phys. Chem.* **1987**, *91*, 2734.
- (17) Sun, Z.; Lou, N.; Nyman, G. *Chem. Phys. Lett.* **2004**, *393*, 204.
- (18) Delmdahl, R. F.; Parker, D. H.; Eppink, A. T. J. B. *J. Chem. Phys.* **2001**, *114*, 8339.
- (19) Kreher, C. J.; Carter, R. T.; Huber, J. R. *Chem. Phys. Lett.* **1998**, *286*, 389.
- (20) Ludowise, P.; Blackwell, M.; Chen, Y. *Chem. Phys. Lett.* **1997**, *273*, 211.
- (21) Zhao, X.; Turco, R. P. *J. Geophys. Res., [Atmos.]* **1997**, *102*, 9447.
- (22) Lawrence, W. G.; Clemishaw, K. C.; Apkarian, V. A. *J. Geophys. Res., [Atmos.]* **1990**, *95*, 18591.
- (23) Richard, E. C.; Vaida, V. *J. Chem. Phys.* **1991**, *94*, 153.
- (24) Richard, E. C.; Vaida, V. *J. Chem. Phys.* **1991**, *94*, 163.
- (25) Delmdahl, R. F.; Bakker, B. L. G.; Parker, D. H. *J. Chem. Phys.* **2000**, *112*, 5298.
- (26) Delmdahl, R. F.; Gericke, K.-H. *Chem. Phys. Lett.* **1997**, *281*, 407.